J Mol Model (2012) 18:4141–4149
DOI 10.1007/s00894-012-1407-2

ORIGINAL PAPER

Molecular modeling of two-photon absorption and third-order nonlinearities of polymethine dyes for all-optical switching

Yuanzuo Li · Ying Shi · Maodu Chen · Yongqing Li · Runzhou Su · Meiyu Zhao · Fengcai Ma

Received: 13 June 2011 / Accepted: 13 March 2012 / Published online: 24 April 2012

Abstract Stimulated by a recent experimental report [Hales JM et al. (2010) Science 327:1485–1488], two-photon absorption and third-order optical nonlinearities of selenopyrylium- and bis(dioxaborine)-terminated polymethine dyes (called SE-7C and DOB-9C) used for all-optical switching were investigated theoretically with time-dependent DFT (TD-DFT) and response theory as well as visualized real-space analysis. The calculated results for the first hyperpolarizability and second hyperpolarizability demonstrated that the two molecules both have large third-order optical nonlinearities. Using real-space analysis, we were able to visually determine that in the one-photon absorption (OPA) process, the first singlet excited state of SE-7C and DOB-9C is an intramolecular charge transfer (ICT) excited state with strong absorption, while the second excited state of these dyes (also termed the "ICT state") shows weak absorption. However, in the two-photon absorption (TPA) process, a larger TPA absorption cross-section was predicted for the second excited state. In this paper, we describe the properties of the S2 excited state, incorporating charge transfer and the transition moment, via real-space analysis, which was very important for understanding the TPA characteristics of the S_2 state.

Keywords Two-photon absorption · Charge transfer · Transition density · Charge difference density

Electronic supplementary material The online version of this article (doi:10.1007/s00894-012-1407-2) contains supplementary material, which is available to authorized users.

Y. Li (✉) · R. Su
College of Science, Northeast Forestry University,
Harbin 150040, People's Republic of China
e-mail: yuanzuo.li@yahoo.com.cn

Y. Shi
Institute of Atomic and Molecular Physics, Jilin University,
Changchun 130012, People's Republic of China

M. Chen
School of Physics and Optoelectronic Technology,
Dalian University of Technology,
Dalian 116024, People's Republic of China

Y. Li · F. Ma
Department of Physics, Liaoning University,
Shenyang 110036, People's Republic of China

M. Zhao
Institute of Theoretical Simulation Chemistry,
Academy of Fundamental and Interdisciplinary Sciences,
Harbin Institute of Technology,
Harbin 150080, People's Republic of China

Introduction

Molecular two-photon absorption [1] (TPA) is currently of great interest because of its applications in various fields, such as optical data storage [2], optical power limitation [3], microfabrication [4], three-dimensional imaging [5], and all-optical switching [6]. TPA occurs in a medium through the simultaneous absorption of two photons via a virtual state; this TPA process complies with even-parity selection rules and shows quadratic intensity dependence [one-photon absorption (OPA) processes exhibit linear intensity dependence and typically conform to odd-parity selection rules). The two-photon absorption coefficient is directly related to the imaginary part of the third-order susceptibility tensor. At the molecular level, the two-photon absorption cross-section of an organic molecule can be characterized by the imaginary part of the molecular third-order nonlinear polarizability, defined at an absorption frequency ω, i.e, $\alpha(\omega) \propto \mathrm{Im}\gamma(-\omega)$. Based on the sum-over-

states (SOS) formalism, it can also be obtained by calculating the TPA transition matrix.

Photon excitation induces electron transfer from the donor group to the acceptor group, followed by changes in the charge density and the transition dipole moment, which are important influences on absorption strength and ability [7–19]. Organic molecules with intramolecular charge-transfer (ICT) properties have been widely studied in the field of nonlinear optics. First, the important discovery that centro-symmetric charge transfer results in a high TPA cross-section led to a general approach to the design of TPA chromophores, with two donor (D) or acceptor (A) terminals linked by a π-conjugated bridge [7]. Recently, Chen et al. successfully synthesized a series of new star-shaped donor-π-acceptor (D-π-A) molecules, all of which exhibited TPA activity in the range 720–880 nm and had large TPA cross-sections that were closely related to the intramolecular charge transfer and the π-conjugation length of the molecule [8]. Some structures of TPA compounds, such as the interesting hyperbranched poly (aroylarylene) and linear poly(aroyltriazole)s (PATAs) [9, 10], are reported to exhibit large TPA values due to their intramolecular charge transfer. Experimental modifications such as increasing the length of conjugation or changing the strengths of the donor and acceptor units have been shown to be useful design strategies for improving charge transfer and absorption performance. The link between TPA (or OPA) and the ICT process has been investigated theoretically for different molecular structures by many researchers [11, 12, 16–25], and some factors (such as the nature of the fragments, the conjugation length, the orientation of the molecule, the molecular dimensionality, and the conformational transitions) exert obvious influences on the optical response of the chromophore. Theoretical research on the OPA and TPA processes may lead to an improved understanding of the nature of charge transfer in OPA and TPA and the microscopic mechanism behind the experimental phenomenon. Recently, Sun et al. developed three-dimensional (3D) representations of the charge-transfer density and transition density in order to study the intramolecular and the intermolecular CT of neutral and charged polymers visually [22, 24], and they successfully used these representations to investigate the TPA process of D-π-A-π-D-type 2,1,3-benzothiadiazoles, based on the quantum chemical results calculated with the semiemparical ZINDO method using the Gaussian 03 program [26]. Though the transition dipole moments between the excited states cannot be obtained with the TD-DFT method using the Gaussian program, the response theory approach implemented in the Dalton program provides a suitable way of obtaining the TPA properties of chromophores, because the contributions from all intermediate states are taken into account in the calculation. Therefore, in our current work, we have combined the results of Dalton with the visualized 3D method in order to investigate the TPA and the OPA of the molecules of interest.

In the work described in this paper, quantum chemistry methods were first used to calculate the strengths of the OPA and the TPA and the third-order nonlinearities of polymethine dyes, which exhibite third-order optical nonlinearities and loss figures of merit [6]. Second, the charge transfer that occurs in the polymethine dyes during OPA and TPA was investigated theoretically utilizing the visualization cube representation of charge transfer, which clearly revealed the orientation of the ground–excited and excited–excited charge transfer. Finally, the 3D transition density was explored in order to study the relationship between its cross-section in OPA and TPA and the transition dipole moment character. Our aim was to reveal the characteristics of the excited states of the two polymethine dyes during OPA and TPA by studying the features of the transition density.

Theoretical methods

All of the quantum chemical calculations were performed with the Gaussian 09 software suite [27]. The ground-state geometries of the selenopyrylium- and bis(dioxaborine)-terminated polymethine dyes (SE-7C and DOB-9C) were optimized using density functional theory (DFT) [28] and Becke's three-parameter hybrid functional with the nonlocal correlation of Lee–Yang–Parr (B3LYP) [29–31]. One-photon absorption (OPA) was examined for the two compounds using the TDDFT method at the B3LYP level, while CAM-B3LYP [32] (which combines the hybrid qualities of B3LYP and long-range correction) was used to check the accuracy of the calculation. TPA calculations were performed at the B3LYP level using the DALTON program [33]. The 6-31G(d) basis set was used for all of the atoms of DOB-9C when calculating the OPA and TPA; for the SE-7C molecule, the 6-31G(d) basis set was used for the C and H atoms, while the aug-cc-pvdz basis set was used for Se. The nonconjugated side chains of the two dyes were repacked with H atoms, because this helped to improve solubility without affecting electronic properties [34].

3D cube representations were utilized to show the orientations and strengths of transition dipole moments and the orientation of charge transfer in the OPA and TPA processes. The allowed excited states for OPA and TPA are the B_u and A_g states, respectively. During photon excitation, the electronic state for dipolar transitions from $\left|\psi_j(B_u)\right\rangle$ to $\left|\psi_k(A_g)\right\rangle_{\pm}$ is written as

$$\begin{aligned}
&{}_{\pm}\left\langle \psi_k(A_g)\right|\vec{\mu}\left|\psi_j(B_u)\right\rangle \\
&= \sum_{m,\mu\in unocc} C_{kmn}(b_g \leftarrow b_g)C_{j\mu o}(a_u \leftarrow b_g)\vec{\mu}_{m\leftarrow u}(b_g \leftarrow a_u) \\
&\pm \sum_{n,o\in occ} C_{kmn}(a_u \leftarrow a_u)C_{j\mu o}(a_u \leftarrow b_g)\vec{\mu}_{n\leftarrow o}(a_u \leftarrow b_g)
\end{aligned} \tag{1}$$

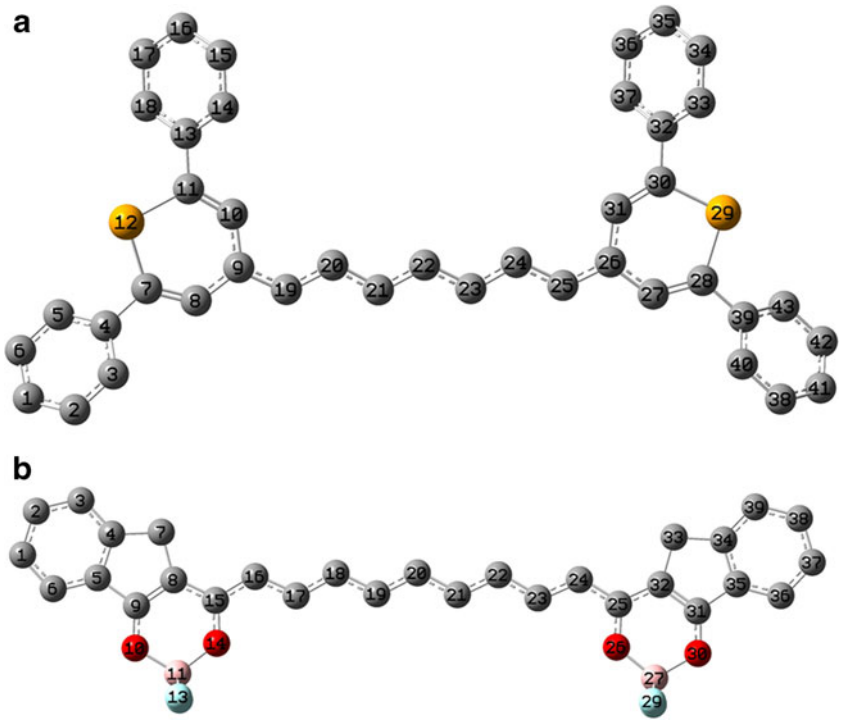

Fig. 1 a-b The chemical structures of SE-7C (**a**) and DOB-9C (**b**)

where $\left|\psi_k(A_g)\right\rangle_-$ and $\left|\psi_k(A_g)\right\rangle_+$ represent the second and higher A_g (two-photon-allowed) excited states [35]. The relationship between the transition dipole moment and the transition density is defined as [36]

$$\mu_{k,j} = e\int \vec{r}\rho_{k,j}(\vec{r})d^3\ \vec{r} \tag{2}$$

Hence, the transition density upon an electronic transition between excited states for TPA is written as

$$\begin{aligned}\rho_{\pm} = &\sum_{m,\mu\in unocc} C_{kmn}(b_g \leftarrow b_g)C_{j\mu o}(a_u \leftarrow b_g)\,\varphi_m\varphi_u \\ \pm &\sum_{n,o\in occ} C_{kmn}(a_u \leftarrow a_u)C_{j\mu o}(a_u \leftarrow b_g)\,\varphi_n\varphi_o\end{aligned} \tag{3}$$

where the $\varphi_n(\varphi_o)$ and $\varphi_m(\varphi_u)$ represent the occupied molecular and unoccupied molecular orbitals. The charge difference density from the excited state j to the excited state k during TPA is written as

$$\Delta\rho_{\pm,kj} = \Delta\rho_{\pm,m,u} \pm \Delta\rho_{\pm,n,o} \tag{4}$$

where $\Delta\rho_{\pm,m,u}$ and $\Delta\rho_{\pm,n,o}$ are

$$\begin{aligned}\Delta\rho_{\pm,m,u} = &\sum_{m,m',\mu\in\text{unocc}} C_{j\mu o}(a_u \leftarrow b_g)C_{kmn}(b_g \leftarrow b_g)C_{km'\text{n}}(b_g \leftarrow b_g)\,\varphi_m\varphi_{m'} \\ - &\sum_{m,\mu,u',\in\text{unocc}} C_{j\mu o}(a_u \leftarrow b_g)C_{j\mu'\text{o}}(a_u \leftarrow b_g)C_{kmn}(b_g \leftarrow b_g)\,\varphi_u\varphi_{u'}\end{aligned} \tag{5}$$

and

$$\begin{aligned}\Delta\rho_{n,o} = &\sum_{n,n'\text{o}\in\text{occ}} C_{kmn}(a_u \leftarrow a_u)C_{km'}(a_u \leftarrow a_u)C_{j\mu o}(a_u \leftarrow b_g)\,\varphi_n\varphi_{n'} \\ - &\sum_{n,o,o'\in\text{occ}} C_{kmn}(a_u \leftarrow a_u)C_{j\mu o}(a_u \leftarrow b_g)C_{j\mu o'}(a_u \leftarrow b_g)\,\varphi_o\varphi_{o'}\end{aligned} \tag{6}$$

The theory behind static electric dipole properties is described in [37]. In the presence of moderate, uniform,

Table 1 Singlet–singlet excitation during OPA for SE-7C

	eV (nm) [a]	CI coefficients [a]	f [a]	nm (f) [b]	nm (f) [c]
S1	1.8072(686.06)	0.54046 (H→L)	2.8964	699.83 (3.01)	685.1 (2.89)
S2	2.5630 (483.74)	0.52020 (H→L+1)	0.0071		
S3	2.7864 (444.97)	0.68579 (H-2→L)	0.1389		
S4	2.8567 (434.01)	0.68412 (H-3→L)	0.1416		
S5	3.0226 (410.19)	0.69091 (H→L+2)	0.0093		

[a] Calculated with TD-B3LYP/6-31G (d)

[b] Calculated with TD-CAM-B3LYP/6-31(d)

[c] Calculated with the Dalton program and the B3LYP functional

Table 2 Singlet–singlet excitation during OPA for DOB-9

	eV (nm) [a]	CI coefficients [a]	f [a]	nm (f)[b]	nm (f)[c]	nm (f)[d]	nm (f)[e]
S1	1.9901(623.00)	0.56313 (H→L)	3.3475	601.78 (3.5282)	616.25 (3.5568)	636.24 (3.4020)	623 (2.780)
S2	2.5843 (479.76)	0.60288 (H→L+1)	0.0036				
S3	3.1007 (399.86)	0.62238 (H→L+2)	0.1802				
S4	3.1958 (387.95)	0.53327 (H-1→L)	0.0070				
S5	3.4138 (363.18)	0.57786 (H→L+4)	0.0007				

[a] Calculated with TD-B3LYP/6-31G (d)

[b] Calculated with TD-CAM-B3LYP/6-31G (d)

[c] Calculated with TD-CAM-B3LYP/6-311+G(d)

[d] Calculated with TD-B3LYP/ 6-311+G(d)

[e] Calculated with the Dalton program and the B3LYP functional

static electric fields in one or more Cartesian direction(s), the total molecular energy can be expressed as a Taylor series:

$$E(F) = E(0) - \mu_i F_i - \frac{1}{2!}\alpha_{ij}F_iF_j - \frac{1}{3!}\beta_{ijk}F_iF_jF_k - \frac{1}{4!}\gamma_{ijkl}F_iF_jF_kF_l - \cdots, \quad (7)$$

where $E(0)$ denotes the energy without external perturbation; the symbols α, β, …, label tensor quantities; and the subscripts indicate Cartesian directions. This expansion is called the "T-convention" [38], and is employed here to determine the static linear polarizability (α), the first hyperpolarizability (β), and the second hyperpolarizability (γ). The Einstein summation convention is used here. The average (hyper)polarizabilities are defined in the following way:

$$\overline{\alpha} = \frac{1}{3}\sum_{i=x,y,z}\alpha_{ij} \quad (8)$$

$$\overline{\beta} = \sum_{i=x,y,z}\frac{\mu_i\beta_i}{|\overrightarrow{\mu}|} \quad (9)$$

where

$$\beta_i = \frac{1}{5}\sum_{j=x,y,z}(\beta_{ijj} + \beta_{jij} + \beta_{jji}) \quad (10)$$

and

$$\overline{\gamma} = \frac{1}{5}\sum_{ij=x,y,z}\gamma_{iijj} \quad (11)$$

The relationship between $\chi^{(3)}$ and γ, the microscopic third-order polarizability, is given by [6]

$$\chi^{(3)} = NL^{(4)}\gamma \quad (12)$$

and

$$\chi^{(3)} = \sqrt{(\mathrm{Re}\chi^{(3)})^2 + (\mathrm{Im}\chi^{(3)})^2} \quad (13)$$

where N and L are the number density and the local factor, respectively, and $\mathrm{Re}(\chi^{(3)})/\mathrm{Im}(\chi^{(3)})=190$ [6].

Results and discussion

The optimized ground-state geometries of SE-7C and DOB-9C with 6-31G(d) can be seen in Fig. 1, where all of the H atoms have been omitted for clarity. We also checked the effect of the basis set by performing calculations with larger basis sets, 6-311+g(d) and 6-311+g(d, p), too. Calculations with 6-311+g(d, p) were not convergent for the two molecules, while the 6-311+g(d) basis set only yielded results for DOB-9C (see the "Electronic supplementary material," ESM). It appears that the choice of basis set has a negligible effect on the structural parameters of DOB-9C; absolute differences in the bond lengths calculated using the different basis sets were within 0.01 Å, and differences in dihedral angles were no larger than 0.1°. Due to the symmetric construction of DOB-9C, the bond lengths and the dihedral angles at symmetric sites should be coherent, and the whole molecule has a planar configuration, as shown in Fig. 1. For

Table 3 Singlet–singlet excitation during TPA for SE-7C, as calculated using the Dalton program and the B3LYP functional

State	eV	nm	Cross-section (10^{-50} cm^4 s photon^{-1})
1	1.81	1366.365	2.449038
2	2.56	968.4823	2697.756
3	2.72	909.2353	505.3496
4	2.79	886.423	599.0125
5	3.05	810.8591	1649.883

Table 4 Singlet–singlet excitation during TPA for DOB-9C, as calculated using the Dalton program and the B3LYP functional

State	eV	nm	Cross-section (10^{-50} cm^4 s photon^{-1})
1	1.99	1242.774	1.044833
2	2.58	958.5737	1248.871
3	3.1	797.7807	91.55982
4	3.2	772.85	8630.5
5	3.41	725.2552	21.39049

SE-7C, calculations showed that the phenyl rings at both ends of the molecule have a twist angle of about 38°.

The calculated electronic transitions for the two molecules during OPA and the TPA are listed in Tables 1, 2, 3, and 4. For DOB-9C, Table 2 shows that the calculated transition energy of the first excited state varies only slightly with the functional employed. The effect of the basis set, including the bigger basis set [6-311+g(d)], on the transition energy was considered, and it was found that varying the basis set had little influence on the results. Moreover, the TDDFT/B3LYP/6-31G method was applied to another polymethine dye (2), and the result (calc.: 633 nm) is closer to the experimental value than the value obtained by the INDO-CIS approach (calc.: 512 nm, data from [15]). The current results therefore accurately reflect the trend in the transition energy for the polymethine system. It is worth noting that we did not check the effect of using a big basis set for SE-7C due to the lack of convergence during ground-state structural optimization.

Table 1 shows that during OPA, the strongest optical absorption of SE-7C corresponds to the first excited state (S1). S3 and S4 are the states with oscillator strength (f)>0.1. The second excited state (S2) yields weak absorption. Based on the TPA results in Table 3, however, the strongest optical absorption is given by S2, and S1 displays only weak absorption. Furthermore, we found similar behavior (i.e., different absorption characteristics during OPA and TPA) for DOB-9C (see Tables 2 and 4). This is a very interesting phenomenon in polymethine dyes with a large third-order optical response.

Table 1 also shows that, for SE-7C, S1 mainly represents the HOMO → LUMO electronic transition (weight: 0.54046), while S2 corresponds to H→L+1 (weight: 0.52020). For DOB-9C, S1 and S2 represent H→L (weight: 0.56313) and H→L+1 (weight: 0.60288), respectively. Generally, frontier molecular orbital analysis, mainly including the electron density of the HOMO and LUMO, can provide valuable information on the charge transfer that occurs upon excitation. Recently, we have developed a method of visualizing the transition density (TD) and the charge difference density (CDD) that accounts for all of the contributions of the molecular orbitals and can be used to study the CT behavior of a π-stacked system [24, 25].

Therefore, in order to elucidate the characteristics of the one- and two-photon spectra of DOB-9C and SE-7C, we used this visualization method to study the two states. Figure 2 shows the transition moment and the charge transfer character using the transition density (TD) and charge difference density (CDD) methods. As shown in Fig. 2, for S1, the total transition dipole moment of SE-7C during OPA consists of a series of small transition dipoles (one per monomeric unit) that cause the phase-coherent transition

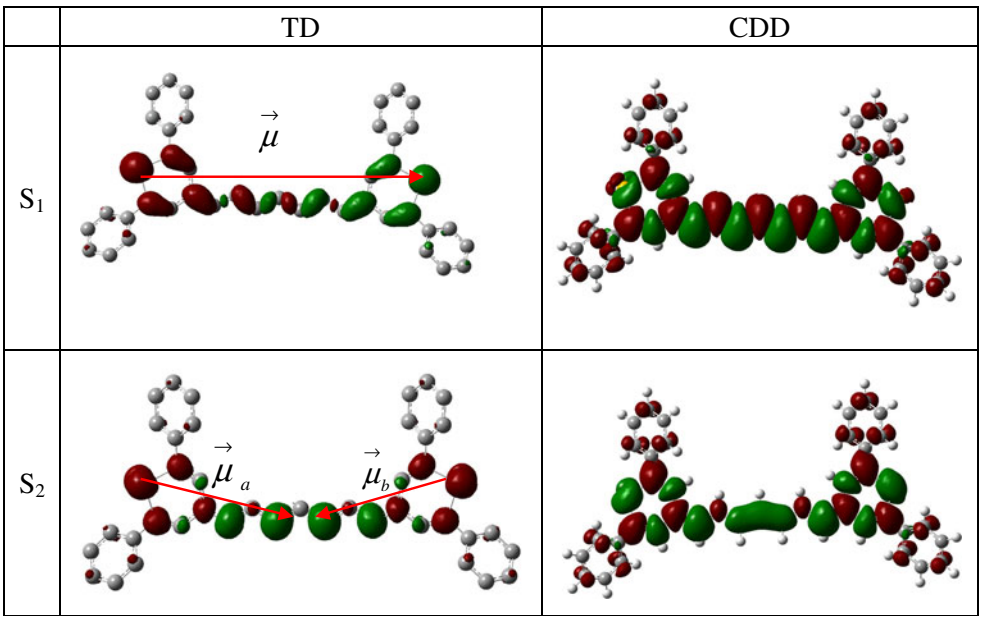

Fig. 2 Transition density (TD) and charge difference density (CDD) for SE-7C during OPA, where *green* and *red* indicate holes and electrons, respectively

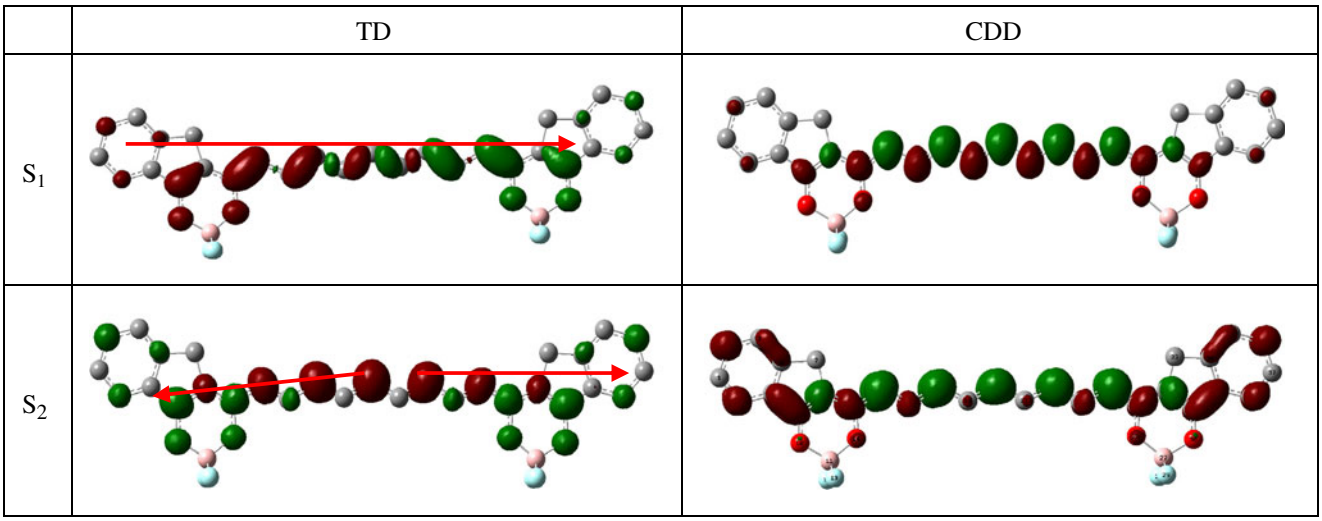

Fig. 3 Transition density (TD) and charge difference density (CDD) for DOB-9C during OPA, where *green* and *red* indicate holes and electrons, respectively

dipole moment, so this state has a single orientated large transition dipole moment. According to the relationship between the oscillator strength and the transition dipole moment, $|\mu|^2 \propto f/E^2$ (where f and E are the oscillator strength and the transition energy), the absorption should be strong. However, for S2 during OPA, there are two sub-transition dipole moments with opposite orientations (i.e., oriented "head to head") for SE-7C, which is bound to weaken the total transition dipole moment, so the total transition dipole moment ($\left|\vec{\mu}_{total}\right| = \left|\vec{\mu}_a + \vec{\mu}_b\right| \approx 0$) is vanishingly small.

For DOB-9C, S1 corresponds to a single orientation of the transition moment from side to side, which means a large value for the oscillator strength. At the same time, S2 has a "tail-to-tail" transition moment, which is opposite to that seen for S2 in SE-7C (see Fig. 3).

The transition probability during TPA can be written as

$$\delta_{tp} = 8\sum_{\substack{lj\neq g \\ j\neq f}} \frac{|\langle f|\mu|j\rangle|^2 |\langle j|\mu|g\rangle|^2}{\left(\omega_j - \omega_f/2\right)^2 + \Gamma_f^2}\left(1+2\cos^2\theta_j\right) + 8 \times \frac{|\Delta_{fg}|^2 |\langle f|\mu|g\rangle|^2}{\left(\omega_f/2\right)^2 + \Gamma_f^2}\left(1+2\cos^2\phi\right) \quad (14)$$

where $|f\rangle$, $|j\rangle$ and $|g\rangle$ are the final, intermediate, and ground states, respectively, θ_j is the angle between the vector $\langle f|\mu|j\rangle$ and $\langle j|\mu|g\rangle$, $\Delta\mu_{fg} = \langle f|\mu|f\rangle - \langle g|\mu|g\rangle$ is the difference between the permanent dipole moments of the excited state and the ground state, and ϕ is the angle between the two vectors $\Delta\mu_{fg}$ and $\langle f|\mu|g\rangle$. In the derivation of Eq. 14, the two-photon resonance condition ($\omega_j = \omega_f/2$) is considered. The first and second terms are called the three-state term and

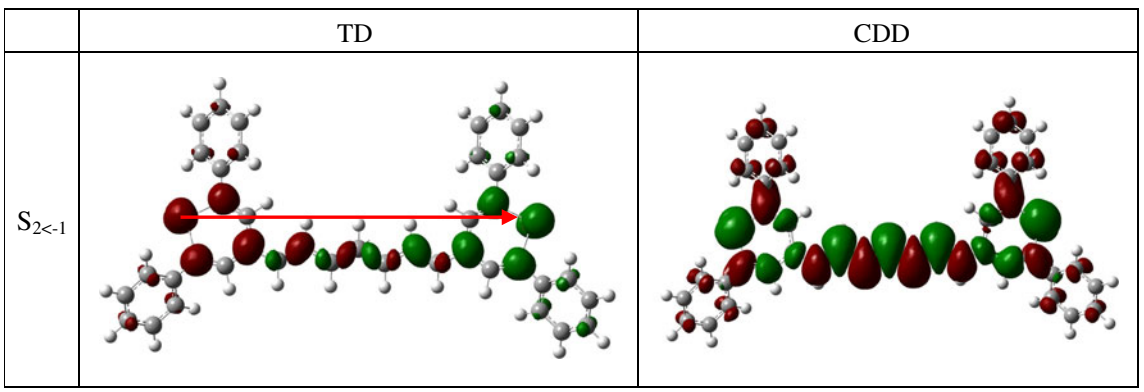

Fig. 4 Transition density (TD) and charge difference density (CDD) for SE-7C during TPA for $S_{2\leftarrow 1}$, where *green* and *red* indicate holes and electrons, respectively

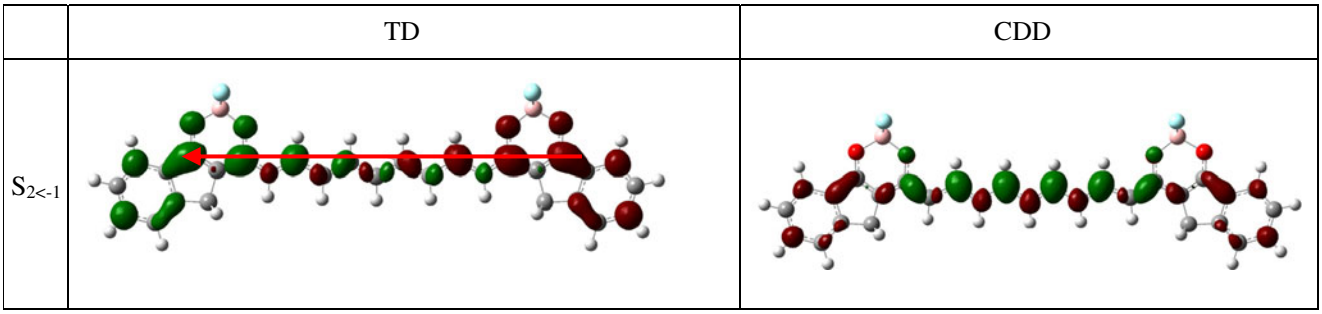

Fig. 5 Transition density (TD) and charge difference density (CDD) for DOB-9C during TPA, where *green* and *red* indicate holes and electrons, respectively

the dipole (two-state) term, respectively. $\Delta\mu_{fg}$ can be obtained by applying a finite field method to the excitation energy.

The calculated two-photon absorption cross-sections of SE-7C and DOB-9C are listed in Tables 3 and 4. It is clear from Table 3 that S2 has a much higher absorption cross-section than S1. The reason for this is the probability of TPA (see Eq. 14). There is no three-state term in Eq. 14 for the first excited state (S1), while the dipole term is vanishingly small for the two centrosymmetric molecules [39] because $\Delta\mu_{fg} = \langle f|\mu|f\rangle - \langle g|\mu|g\rangle \approx 0$, which leads to the weak absorption cross-section of S1. If we consider $S_{2\leftarrow1}\leftarrow S_{1\leftarrow0}$ for SE-7C and DOB-9C during TPA, the three-state term in Eq. 14 becomes the most important term according to the TPA transition rule, and this dipole moment term is very small for a centrosymmetric molecule. It is clear from Figs. 2 and 4 that θ_j is zero for SE-7C, considering the parallel orientation of the transition dipole moments of $\langle 2|\mu|1\rangle$ and $\langle 1|\mu|0\rangle$. For DOB-9C, θ_j is 180° (see Figs. 3 and 5), so $\cos^2\theta_j = 1$. Furthermore, the transition densities also demonstrate that $\langle 2|\mu|1\rangle$ and $\langle 1|\mu|0\rangle$ are both large and have similar transition moment character, which results in a large TPA absorption cross-section.

Charge difference densitys allow us to follow the change in the static charge distribution upon excitation during OPA and TPA. In OPA, the charge difference density (see Fig. 2) for S1 in SE-7C revealed that the electron–hole pairs are delocalized on selenopyrylium and polymethine, and that the four benzenyl rings are electron acceptors, since more electrons are localized in the terminal benzenyl rings, while green holes reside in the middle chain. During TPA, the charge difference density (see Fig. 4) for $S_{2\leftarrow1}$ revealed that the charge distribution on excitation is similar to that seen for S1 during OPA, so the state is also an ICT state where electrons are transferred from the middle chain to the terminal group. For DOB-9C, the charge difference density for S1 in Fig. 3 shows that most of the electrons and holes are delocalized on the polymethine chain in an alternating distribution; while S2 during OPA is an ICT state in which most of the holes are localized on the polymethine chain and most electrons are localized on the bis(dioxaborine). Similarly, the charge transfer density of $S_{2\leftarrow1}$ during TPA indicates that it is also an ICT state (see Fig. 5).

The calculated average (hyper)polarizabilities are listed in Table 5, which shows that the values of the static linear polarizability (α), the first hyperpolarizability (β), and the second hyperpolarizability (γ) for SE-7C are larger than those for DOB-9C. It is worth noting that the value of Re($\chi^{(3)}$) for Se-7C was calculated as -8.07×10^{-32} esu, which is very similar to the -2.2×10^{-31} esu reported in [6]. Moreover, DOB-9C also has a large value of Re($\chi^{(3)}$), 4.08×10^{-32} esu. Therefore, the two molecules have large third-order optical nonlinearities. Based on its values for the first and second hyperpolarizability, Se-7C displays greater nonlinear character than DOB-9C.

Conclusions

The TPA and third-order optical nonlinearities of SE-7C and DOB-9C have been investigated theoretically using DFT and TD-DFT in combination with visualization methods (TD and CDD). The transition density (TD) shows the orientation and strength of transition dipole moments from the ground state to the excited state and transition dipole moments between the excited states, while the charge difference density (CDD) revealed the orientation and results of charge transfer. Using the visualization method, we found that the first excited state of SE-7C and DOB-9C is an intramolecular charge transfer state, that it has the greatest

Table 5 Data on nonlinear components for SE-7C and DOB-9C

Molecule	$\overline{\alpha}^a$	$\overline{\beta}^a$	$\overline{\gamma}^a$	Re($\chi^{(3)}$) (esu)
Se-7C	1117.03	−8610.98	−215638.63	-8.73×10^{-32}
DOB-9C	917.01	−6044.92	100684.38	4.08×10^{-32}

* All values are given in atomic units

oscillator strength, and that it involves the transfer of an electron from the middle chain of the polymethine dye to the terminal group. Meanwhile, we also found that during TPA, the second excited state has the largest absorption cross-section, due to the large state-to-state transition moment. The calculated nonlinear parameter indicated that SE-7C exhibits a stronger nonlinear optical response than DOB-9C.

Acknowledgments This work was supported by the National Natural Science Foundation of China (grants 10874234, 90923003, 10804015) and the Fundamental Research Funds for the Central Universities (grant no: DL12BB19).

References

1. Göppert-Mayer M (1931) Über Elementarakte mit zwei Quantensprüngen. Ann Phys 401:273–294
2. Parthenopoulos DA, Rentzepis PM (1989) Three-dimensional optical storage memory. Science 245:843–845
3. Ehrlich JE, Wu XL, Lee YS, Hu ZY, Röckel H, Marder SR, Perry JW (1997) Two-photon absorption and broadband optical limiting with bis-donor stilbenes. Opt Lett 22:1843–1845
4. Cumpston BH, Ananthavel SP, Barlow S, Dyer DL, Ehrlich JE, Erskine LL, Heikal AA, Kuebler SM, Lee YS, McCord Maughon D, Qin J, Röckel H, Rumi M, Wu XL, Marder SR, Perry JW (1999) Two-photon polymerization initiators for three-dimensional optical data storage and microfabrication. Nature 398:51–54
5. Denk W, Strickler JH, Webb WW (1990) Two-photon laser scanning fluorescence microscopy. Science 248:73–76
6. Hales JM, Matichak J, Barlow S, Ohira S, Yesudas K, Brédas JL, Perry JW, Marder S (2010) Design of polymethine dyes with large third-order optical nonlinearities and loss figures of merit. Science 327:1485–1488
7. Albota M, Beljonne D, Bredas JL, Ehrlich JE, Fu JY, Heikal AA, Hess SE, Kogej T, Levin MD, Marder SR, McCord-Maughon D, Perry JW, Rockel H, Rumi M, Subramaniam G, Webb WW, Wu XL, Xu C (1998) Design of organic molecules with large two-photon absorption cross sections. Science 281:1653–1656
8. Zou L, Liu ZJ, Yan XB, Liu Y, Fu Y, Liu J, Huang ZL, Chen XG, Qin JG (2009) Star-shaped D-π-A molecules containing a 2,4,6-tri (thiophen-2-yl)-1,3,5-triazine unit: synthesis and two-photon absorption properties. Eur J Org Chem 32:5587–5593
9. Qin AJ, Lam JWY, Dong HC, Lu WX, Jim CKW, Dong YQ, Häubler M, Sung HHY, Williams ID, Wong GKL, Tang BZ (2007) Metal-free, regioselective diyne polycyclotrimerization: synthesis, photoluminescence, solvatochromism, and two-photon absorption of a triphenylamine-containing hyperbranched poly (aroylarylene). Macromolecules 40:4879–4886
10. Qin AJ, Jim CKW, Lu WX, Lam JWY, Häubler M, Dong YQ, Sung HHY, Williams ID, Wong GKL, Tang BZ (2007) Click polymerization: facile synthesis of functional poly(aroyltriazole)s by metal-free, regioselective 1,3-dipolar polycycloaddition. Macromolecules 40:2308–2317
11. Martin RL (2003) Natural transition orbitals. J Chem Phys 118:4775
12. Fang YR, Li YZ, Xu HX, Sun MT (2010) Ascertaining *p,p′*-dimercaptoazobenzene produced from *p*-aminothiophenol by selective catalytic coupling reaction on silver nanoparticles. Langmuir 26:7737–7746
13. Krueger BP, Scholes GD, Fleming GR (1998) Calculation of couplings and energy-transfer pathways between the pigments of LH2 by the ab initio transition density cube method. J Phys Chem B 102:5378–5386
14. Cho BR, Son HK, Lee SH, Song YS, Lee YK, Jeon SJ, Choi JH, Lee H, Cho M (2001) Two photon absorption properties of 1,3,5-tricyano-2,4,6-tris(styryl)benzene derivatives. J Am Chem Soc 123:10039–10045
15. Matichak JD, Hales JM, Ohira S, Barlow S, Jang SH, Jen AKY, Bredas JL, Perry JW, Marder SR (2010) Using end groups to tune the linear and nonlinear optical properties of bis(dioxaborine)-terminated polymethine dyes. Chem Phys Chem 11:130–138
16. Wang XF, Zhang XR, Wu YS, Zhang JP, Ai XC, Wang Y, Sun MT (2007) Two-photon photophysical properties of tri-9-anthrylborane. Chem Phys Lett 436:280–286
17. Li MY, Hao R, Fu LM, Su WJ, Zhao XH, Zhang JP, Ai XC, Sun MT, Wang Y (2007) Spectroscopic and theoretical studies on the photophysical properties of dichlorotriazine derivatives. Chem Phys Lett 444:297–303
18. Amadei A, D'Abramo M, Nola AD, Arcadi A, Cerichellic G, Aschi M (2007) Theoretical study of intramolecular charge transfer in π-conjugated oligomers. Chem Phys Lett 434:194–199
19. Haiss W, Zalinge HV, Bethell D, Ulstrup J, Schiffrina DJ, Nicholsa RJ (2006) Thermal gating of the single molecule conductance of alkanedithiols. Faraday Discuss 131:253–264
20. Nguyen KA, Day PN, Pachter R (2008) Effects of conjugation in length and dimension on two-photon properties of fluorene-based chromophores. Theor Chem Acc 120:167–175
21. Wang CK, Zhao K, Su Y, Luo Y, Ren Y, Zhao X (2003) Solvent effects on the electronic structure of a newly synthesized two-photon polymerization initiator. J Chem Phys 119:1208
22. Sun MT, Kjellberg P, Beenken WJD, Pullerits T (2006) Comparison of the electronic structure of PPV and its derivative DIOXA-PPV. Chem Phys 327:474–484
23. Beenken WJD, Pullerits T (2004) Spectroscopic units in conjugated polymers: a quantum chemically founded concept? J Phys Chem B 108:6164–6169
24. Li YZ, Pullerits T, Zhao MY, Sun MT (2011) Theoretical characterization of the PC60BM:PDDTT mode for an organic solar cell. J Phys Chem C 115:21865–21873
25. Li YZ, Li HX, Zhao XM, Chen MD (2010) Electronic structure and optical properties of dianionic and dicationic π-dimers. J Phys Chem A 114:6972–6977
26. Sun MT, Chen JN, Xu HX (2008) Visualizations of transition dipoles, charge transfer, and electron–hole coherence on electronic state transitions between excited states for two-photon absorption. J Chem Phys 128:064106
27. Frisch MJ, Trucks GW, Schlegel HB, Scuseria GE, Robb MA, Cheeseman JR, Scalmani G et al (2009) Gaussian 09, revision A.02. Gaussian Inc., Wallingford
28. Dreizler JMR, Gross EKU (1990) Density functional theory. Springer, Heidelberg
29. Becke AD (1988) Density-functional exchange-energy approximation with correct asymptotic behavior. Phys Rev A 38:3098–3100
30. Becke AD (1993) Density–functional thermochemistry. III. The role of exact exchange. J Chem Phys 98:5648
31. Lee C, Yang W, Parr RG (1998) Development of the Colle–Salvetti correlation-energy formula into a functional of the electron density. Phys Rev B 37:785–789
32. Yanai T, Tew DP, Handy NC (2004) A new hybrid exchange-correlation functional using the Coulomb-attenuating method (CAM-B3LYP). Chem Phys Lett 393:51–57
33. Helgaker T et al. (2012) DALTON, release 2.0: an ab initio electronic structure program. http://www.kjemi.uio.no/program/dalton/dalton.html
34. Tolbert LM (1992) Solitons in a box: the organic chemistry of electrically conducting polyenes. Acc Chem Res 25:561–568

35. Ohta K, Kamada K (2006) Theoretical investigation of two-photon absorption allowed excited states in symmetrically substituted diacetylenes by ab initio molecular-orbital method. J Chem Phys 124:124303
36. Beenken WJD, Pullerits T (2004) Excitonic coupling in polythiophenes: comparison of different calculation methods. J Chem Phys 120:2490
37. Loboda O, Zalesny R, Avramopoulos A, Luis JM, Kirtman B, Tagmatarchis N, Reis H, Papadopoulos MG (2009) Linear and nonlinear optical properties of [60]fullerene derivatives. J Phys Chem A 113:1159–1170
38. Willets A, Rice JE, Burland DM, Shelton DP (1992) Problems in the comparison of theoretical and experimental hyperpolarizabilities. J Chem Phys 97:7590–7599
39. Fu J, Padilha LA, Hagan DJ, Van Stryland EW, Przhonska OV, Bondar MV, Slominsky YL, Kachkovski AD (2007) Molecular structure—two-photon absorption property relations in polymethine dyes. J Opt Soc Am B 24:56–66